

### Association of Arab Universities Journal of Engineering Sciences

مجلة اتحاد الجامعات العربية للدراسات والبحوث الهندسية



### Effect of Gates Operation on Maximum Scour Downstream of Kahlaa Regulator

Hadi Ameer Abbas 1,\*, and Hayder Q. Majeed 2

- <sup>1</sup> Department of Water Resources Engineering, College of Engineering, University of Baghdad, Baghdad, Iraq, Hadi.ameer2310 @coeng.uobaghdad.edu.iq
- <sup>2</sup> Department of Water Resources Engineering, College of Engineering, University of Baghdad, Baghdad, Iraq, hmajeed @coeng.uobaghdad.edu.iq
- \* Corresponding Author: Hadi Ameer Abbas Hadi.ameer2310 @coeng.uobaghdad.edu.iq

Published online: 30 September 2025

Abstract— Regulators and other hydraulic structures are crucial for managing flow in open channels. Unpredictable scour patterns are produced when such structures' gates are operated improperly. The purpose of the study is to look into the optimal functioning of the Al-Kahlaa Regulator's gates in Iraq, focusing on sediment movement and sedimentation issues. In this research, Flow-3D software, specifically the turbulent RNG model, was used to simulate water flow and sediment scour theory to simulate sediment movement under different flow conditions and gate opening options. According to the study, the number of open gates and how they are operated have a big impact on how scour develops downstream of the regulator. The maximum scour depth value was recorded when one gate was opened, which was 13-times more compared to the case when all gates were opened for the flow rate of 125 m³/s. On the other hand, in case of one gate was opened the maximum scour depth was recorded at 2.05 m when the rate of flow was 50 m³/s and 3 m at 200 m³/s, equivalent to 1.5 times increase. In general, the maximum scour depth downstream of the regulator decreases as the number of open gates increases. Therefore, the most favorable operating scenario is when all gates are open, while the worst scenario is when only one gate on side is open.

Keywords—Al-Kahlaa Regulator, Flow-3D, Open channel flow, RNG model, Scouring.

#### 1. Introduction

The removal of soil particles from the channel bed and banks as a result of water action is known as scour. It happens as a result of the channel's natural water flow changing or as a result of human activities, including dredging of bed material or building within the waterway [11]. Any hydraulic structure's local scour downstream is thought to be the most potent occurrence that could impair the structure's performance. Since the cost of protecting the entire structure from scour is high, it is necessary to predict both the maximum depth of scour and the upstream slope of the scour hole in order to reduce maintenance expenses and failure risk [20].

Multievents are seen in a number of current hydraulic structures, including regulators. Basically, a large portion of the issues with these structures downstream are caused by the multievent improper operation, which results in erratic scour patterns. One of the following scenarios could result in inadequate operation: improper observance of the necessary operating rules. Periodic maintenance of the gates and their mechanical equipment is inadequate When severe scour patterns happen downstream of certain structures, failures of these structures, or any portion of them, are expected. The maximum dimensions of the resulting scour hole must be predicted in advance for the regulators to be designed appropriately [11]. The regulator serves primarily as a crucial component in the channel system that transfers river water for agriculture and other beneficial uses. Many of the hydraulic facilities in Iraq are

used including regulators, have had issues with scouring both upstream and downstream as a result of improper multi-opening operations, which produce peculiar scour patterns.

Therefore, the management and operation of water resource projects directly and significantly affect the most efficient use of water [20]. The hydraulic properties of unsteady flow in rivers must be specified by hydraulic model simulations in order to identify problems and recommend appropriate remediation measures [9]. The gates' and their mechanical devices' insufficient and irregular maintenance, as well as a strict and defined routine operation rule that is followed, may lead to improper operation in such hydraulic systems. Around the world, numerous structures have collapsed as a result of severe dredging. Thus, after crushing, the safety of the current facility primarily rests on the ongoing observation of local scour [24].

The local scour depth and sediment accumulation could be influenced by a range of particular factors. The characteristics of particle, rate of flow, flow time, Froude Number, operating regime, and gate opening sequence are the most important ones to consider when analyzing the parameters that will be investigated for their impact on the scourdownstream the regulator under various flow rates.

Many researchs utilized mathematical models to investigate the impact of flow conditions on the scour depth at hydraulic structures by using various software such as HEC-RAS, Ansys Fluent and 3D flow. Using HEC-RAS model, [26] evaluated the impact of floating debris on local scour at bridge piers and determined the varation of scure hole shape and depth under various flow conditions. [1] developed a mathematical model in their study and used it to examine the Samarra-Al Tharthar system hydraulically. They showed that sediment accumulates and forms islands upstream of regulators at low velocities. The system's efficiency is reduced, and its structural stability is threatened by these islands and sedimentation. [2] investigate the behavior of the scouring pattern between bridge piers under particular hydraulic circumstances was investigated. They observed in their study that the scour depth rises over time, sediments are carried away from the scour site, and erosion continues until equilibrium is reached. Mobile bed scour, where sediment is transported from the inflow load, initially increases and varies over time. Equilibrium occurs when transported sediment equals removed sediment [17] created for the purpose of conducting a numerical simulation of the operational impact of the Al-Hay Regulator's gate openings on local erosion, they found that increasing the Froude Number results in more soil removal and scour depth around the regulator. The depth of scour depends on gate numbers, order, and operation system. Unevenly distributed or open gates increase scouring depth. [3] utilized 3D CFD-based model to investigate the impact of rectangular debris accumulation around single and dual cylindrical piers on river bed morphology under

clear water conditions. The influence of flow characteristics on scour hole shape and depth, as well as the average velocity were determined and assessed.

[6] investigated the velocity patterns in the reservoir using different operating techniques for the planned Makhool Dam. Because the velocity values were lower than those obtained by operating successive gates with the same discharge, the study concluded that operating nonconsecutive gates was the best course of action. A more appropriate velocity distribution is produced by operating gates with more openings and fewer numbers with a specific outflow than by running gates with fewer openings and more numbers with the same outflow.

As for laboratory research conducted recently, it was created by [14] experimentally investigated many conditions surrounding local scour around curved groynes. The study revealed that, although significant, the Froude Number does not dominate the processes governing scour and sediment movement and the scouring amount and flow velocity are directly correlated with the Froude Number, even when all other factors remain constant. [16] conducted a laboratory study to demonstrate the extent to which the operation of the barrage gates affects the maximum depth of scouring downstream of the dam and reached results, the most important of which is that the maximum depth of erosion is greatly affected by the arrangement and number of open gates. [3] conducted experimental investigation the impact of debris jams on scour depth at cylindrical bridge piers and compared the primary known empirical models. A total of 27 experiments on rectangular geometry were conducted across three distinct groups based on width, length, submerged depth, and blocked area. The findings indicated that the buildup of debris increased scour depth. [4] state that the size of the bed material directly affects how sediments are transported. They created a lab experiment, and according to their research, the diameter of the scour hole, the maximum level of scour volume, and the scour process itself are all highly influenced by grain size. They concluded that the highest depth and area of scour decreased as the median size, d50, and geometric standard deviation increased. [22] They looked into how well silt was removed from reservoirs by considering the effects of sediment nonuniformity, slit weir diameters, weir slit position, and discharge. It was discovered that, in comparison to finer material, coarser sediment reduces scour volume by a factor of 22. Regardless of bed material nonuniformity, the study investigated five alternative slit weir dimensions and discovered that a three-fold increase in discharge correlates to a ten-fold increase in scour volume. [5] studied the complex dynamics of local scour around Bridge piers considering the impact of near surface and surface debries.

The current study uses Flow-3D software to create a mathematical model that simulates sediment transport within the Al-Kahlaa Regulator's reach, taking into account the effects of increasing flow rate, the number of

gates opening, and the order in which the gates open. Additionally, determine the proper gate opening operation to lessen scouring downstream of the regulator structure.

#### 2. Mathematical Model

Volume of Fluid (VOF) and the fractional area volume obstacle representation techniques (FAVOR<sup>TM</sup>) are used by Flow Science Inc.'s Flow-3D v11.2 program to determine the free surface and any obstacles in its path. This guarantees the tracking of the liquid/gas contact and the realistic representation of the dynamics of the free surface. [12] Flow-3D comprises the function of fluid volume, the transport equation, and the boundary conditions as its three primary parts [10].

The FLOW-3D program employs VOF method to model free surface flow in simulation. In order to obtain precise free surface conditions for the VOF method, the program must fulfill three requirements:

- 1 The fraction variable (F) must be determined for every individual cell. In the case of F=1, it means that the cells are totally filled with fluid, while When F=0, it refers to the empty cell.
- 2 -Achieving an adequate free surface is crucial. It is possible to achieve the free surface appropriately as F is computed for each cell.
- 3- Boundary conditions can be considered another essential factor. The method of VOF requires six boundaries conditions Which be defined in the program.

#### 2.1 formulation and Theory of CFD Model

The Reynolds-Averaged Navier-Stokes (RANS) equation is used to model the movement of an incompressible viscous fluid. It describes in detail how viscous fluid substances move in three dimensions within the Flow-3D software. The equations governing the fluid velocity in the x-, y-, and z-coordinates (u, v, and w) are referred to as the motion equations that can be given

$$\begin{split} \frac{\partial u}{\partial t} &+ \frac{1}{v_F} \left( u A_x \frac{\partial u}{\partial x} + v A_y \frac{\partial u}{\partial y} + w A_z \frac{\partial u}{\partial z} \right) = -\frac{1}{\rho} \frac{\partial p}{\partial x} + \\ G_x &+ f_x \\ \frac{\partial v}{\partial t} &+ \frac{1}{v_F} \left( u A_x \frac{\partial v}{\partial x} + v A_y \frac{\partial v}{\partial y} + w A_z \frac{\partial v}{\partial z} \right) = -\frac{1}{\rho} \frac{\partial p}{\partial y} + \\ G_y &+ f_y \\ \frac{\partial w}{\partial t} &+ \frac{1}{v_F} \left( \frac{u A_x \partial w}{\partial x} + v A_y \frac{\partial w}{\partial y} + w A_z \frac{\partial w}{\partial z} \right) = -\frac{1}{\rho} \frac{\partial p}{\partial z} + \\ G_z &+ f_z \end{split}$$

$$(1)$$

The variables in the equation are defined as follows:  $V_F$  denotes the proportion of volume, Ai represents the proportion of the area,  $\rho$  represents the fluid density, p represents the average hydrodynamic pressure, the symbols Gi denote the acceleration of the body and  $f_i$  acceleration due to viscosity.

#### 2.2 model of Turbulence

Turbulence is the absence of a stabilizing force and is typified by oscillations at high frequencies and the creation of different eddies with varying energy [10]. Turbulence refers to the disordered and unpredictable movement of a fluid, based on the Reynolds number. High Reynolds numbers cause the emergence of eddies with different length scales due to the flow's inherent instability.

The Flow-3D software provides a selection of six turbulent flow models. The recommended topics encompass Prandtl mixing length, one-equation, two-equation, renormalized group, and large eddy simulation.

Flow-3D software is commonly employed in numerous studies to replicate sediment scour, and the renormalized group model is the prevailing choice for this purpose. This model provides an accurate description of low-intensity turbulent flow, particularly in areas with a greater shear zone. The computational efficiency of this model surpasses that of Large Eddy Simulation (LES). which necessitates a smaller mesh size. This is the reason it was chosen for the studies conducted by [31] and [23]. Using statistical methods, the renormalized group k-ε turbulence model [30] and [27] generated averaged formulas for turbulence parameters, including the rate at which turbulent kinetic energy dissipates. This model is more widely applicable than the k-ε model since it makes use of equations that are similar to it; nonetheless, the turbulent model RNG k-ε generates the equation constants explicitly. It's governed by the following equations:

$$\frac{\partial k_T}{\partial t} + \frac{1}{V_F} \left( u A_x \frac{\partial k_T}{\partial x} + v A_y \frac{\partial k_T}{\partial y} + w A_z \frac{\partial k_T}{\partial z} \right) = P_T + G_T + D_i f f_{kT} - \varepsilon_T$$
 (2)

$$\frac{\partial k_{T}}{\partial t} + \frac{1}{V_{F}} \left( u A_{x} \frac{\partial k_{T}}{\partial x} + v A_{y} \frac{\partial k_{T}}{\partial y} + w A_{z} \frac{\partial k_{T}}{\partial z} \right) = \frac{CDIS1 \cdot \varepsilon_{T}}{k_{T}} \left( P_{T} + CDIS3 \cdot G_{T} \right) + D_{i} f f_{\varepsilon} - CDIS2 \frac{\varepsilon^{2}_{T}}{k_{T}} \varepsilon_{T}$$
(3)

where  $P_T$  generation of chaotic kinetic energy,  $G_T$  Generation of turbulent buoyancy,  $k_T$  is turbulent kinetic energy refers to the distinct form of kinetic energy connected to variations in turbulent flow velocity (turbulent kinetic energy)  $A_z$ ,  $A_y$ ,  $V_F$ , and  $A_x$  are the FAVOR functions, and the terms  $D_i f f_{kT}$  and  $D_i f f_{\varepsilon}$  Express the phrases that describe the spreading and dissipation of turbulent kinetic energy, while  $\varepsilon_T$  Turbulent dissipation rate refers to the speed at which turbulent energy is lost or dissipated. The dimensionless parameters *CDIS1*, *CDIS2*, and *CDIS3*, the user has the ability to modify the parameters, which default to 1.44, 1.92, and 0.2.

#### 2.3 model of Sediment Scour

A technique for predicting the erosion, sedimentation, and deposition of packed and suspended sediments is the sediment scour model. [31] and [15].

According to [27], The physical properties of packed and suspended sediments, encompassing processes such as transport, erosion, sedimentation, and accumulation, are predicted using sediment scour models. The models include drift, scour, bed-load transfer, and deposits. Sediment moves with the river, settles due to gravity, and gets caught in the water's flow. When Sediment undergoes rolling and sliding movements down the packed bed surface as a result of fluid flow shear stress, bed-load transfer takes place. Gravity, buoyancy, and friction cause deposits to settle and solidify. The key variables in the model consist of the critical Shields number, the equation for bed load transit rate, the highest rate of packing, the shear stress in bed, and the characteristics of the sediment.

The critical shear stress  $\tau_{cr}$ , required to dislodge sediment particles from the surface of the compacted bed, is directly related to the critical shields value  $\theta_{cr,i}$  [8]. Sediment erosion is a possible occurrence based on factors such as the size, density, and external pressures acting on the silt [27].

$$\theta_{cr,i} = \frac{\tau_{cr,i}}{gd_i(\rho_i - \rho_f)} \tag{4}$$

The variables in question are: g which denotes the magnitude of gravity,  $d_i$  which represents the size of sediment grains and  $\rho_i$  and  $\rho_f$ , which stand for the mass density of sediment grains and the density of the fluid, respectively.

The Flow-3D software calculates the critical Shields number  $\theta_{cr,i}$  using either a predefined value computed internally or a calculated value obtained from the Soulsby-Whitehouse equation shown below [28].

$$d_{*,i} = d_i \left[ \frac{g(s_i - 1)}{\vartheta_f} \right]^{\frac{1}{3}} \tag{5}$$

$$\theta_{cr,i} = \frac{0.3}{1 + 1.2 d_{*,i}} + 0.055 \left[ 1 - \exp(-0.02 d_{*,i}) \right]$$
 (6)

The variable  $d_{*,i}$  represents the dimensionless grain size,  $\vartheta_f$  refers to the fluid's kinematic viscosity, whereas  $s_i$  reflects the ratio of the density of the grains to the density of the fluid.  $\theta_{cr,i}$  could be set to a default value of 0.05, as suggested by [29].

Transport of bed loads the process of transporting sediment by either rolling or bouncing it across the surface of a densely packed sediment bed is called  $\Phi$ i. The Flow-3D program knows three distinct formulas that can be used

to get the volumetric sediment transfer rate per bed width: 1- Müller, Peter, and Meyer formula

$$\Phi i = \beta_{MPM,i} (\theta_i - \theta'_{cr,i})^{1.5} c_{b,i} \tag{7}$$

where  $\beta_{MPM,i}$  is the coefficient of bed load can reach 13.0 for extremely high transport, 5.0 to 5.7 for moderate transport, and 8.0 for low transport [19].

2-Nielsen formula [21]

$$\Phi i = \beta_{Nie,i} \theta_i^{0.5} (\theta_i - \theta'_{cr,i}) c_{b,i}$$
 (8)

where  $\beta_{Nie,i}$  is known as the coefficient of bed load, and the default setting is 12.0.

3-Van Rijn formula [25]

$$\Phi i = \beta_{VR,i} \theta d_{*,i}^{-0.3} (\frac{\theta_i}{\theta'_{rr,i}} - 1)^{2.1} c_{b,i}$$
(9)

where the standard alue of the coefficient of bed load  $\beta_{VR,i}$  is 0.053. Consequently, the volume fraction of species I in the bed material is represented by  $c_{b,i}$  in all mathematical expressions.

#### 2.3.1 Physics

To provide accurate simulations of the data needed for this investigation, just four of the various physics options must be chosen. When the gravitational acceleration in the vertical, or z-direction, is adjusted to - 9.81 m/sec², the gravity option. The option of turbulence and viscosity is enabled by imposing Newtonian viscosity on the flow and choosing a suitable turbulence model. After the FLOW-3D model was finished being constructed, one turbulence model may be used in this investigation as long as the renormalized group (RNG) model was selected. The sediment scour model was activated and was set to median diameter and density.

#### 2.3.2 Sediment Properties

Before using the Flow-3D program to model sediment scour, the user needs to determine the exact properties of the sediment, depending on the real circumstances. The entrainment coefficient, which has a preset value of 0.018, regulates how quickly the bed material erodes. It also determines how quickly the particles rise to the surface and fall off of the packed bed. The angle of repose parameter determines how much the local critical shielding value is changed, typically ranging from 30 to 40 degrees, with 32 degrees as the default. This parameter takes into consideration the maximum bed slope angle at which grains start to slide on their own [10].

Two additional parameters and settings are Bed Shearing Stress and Max Packed Portion. The Maximum Packing Fraction represents (1-porosity), the cell's open volume and the combined volume of all particle species. A sand's maximum packed portion ranges from 0.55 to 0.7 when its porosity falls between 0.3 and 0.45. The number by default is 0.64. In terms of the bed shear stress, the standard wall function for three-dimensional turbulent flow is used to calculate the fluid's shear force on the packed bed's surface, accounting for the roughness of the wall. By dividing the median grain diameter  $d_{50}$  in packed sediment by the Nikuradse roughness ks, one can determine the Crough coefficient, which is user adjustable. For simulations involving many species, the default value of this coefficient is 2.5; for simulations involving a single species, it is 1.0. [10]

#### 2.4 model of Sediment Scour

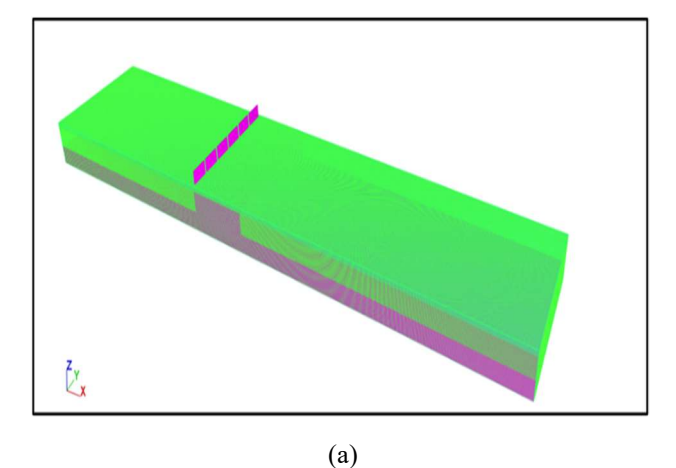
It is important to define fluid properties like density, temperature, and viscosity precisely. While fluid properties can be set on the Fluids tab, the fluid can be selected based on the fluid database tab. To aid the user, FLOW-3D includes a library of widely available resources. Depending on the Meshing and Geometry tab, each component's solid characteristics can be defined. In the present investigation, water at 20°C is chosen.

#### 2.5 Geometry

The AutoCAD-3D modeling tool is used to draw the 3D solid geometry of the model. The geometry used in the simulations is exported as a stereolithographic (.stl) format that Flow 3D from AutoCAD can recognize, depending on the information available from the field data. After that, the STL files are directly imported into FLOW 3D as shown in **Figure 1**, allowing for the generation of the necessary mesh

#### 2.6 Meshing

The creation of a grid is crucial for achieving an exact solution in numerical models. A precise mesh quality is essential for producing realistic results. The choice of grid and cell size significantly impacts the accuracy of results and simulation time. The ideal cell size should be estimated by starting using a big mesh and progressively shrinking the size until the output remains consistent as shown in Figure 1, therefore, different cell sizes are selected as (1, 0.75, 0.5, 0.3 and 0.20) m to identify the best cell size that satisfy the phenomenon conditions. The mesh size of (0.3 m) is used in this study as a best when the comparison was made among the output results. Increasing the number of cells can slow down computation, so it is essential to select the ideal cell count. Flow-3D allows for the specification of orthogonal meshes using either cylindrical or cartesian coordinates. The FAVOR option is reliable for obtaining the optimal cell count. Each cell's aspect ratio must not exceed 3:1 in any two dimensions, and the ratio between neighboring cells must not exceed 1.25 in the same direction. It is recommended to use cells with a 1:1 size ratio to achieve the best results, and a mesh configuration between each block should not exceed a 2:1 ratio [13], as shown in Figure 1, allowing for the generation of the necessary mesh



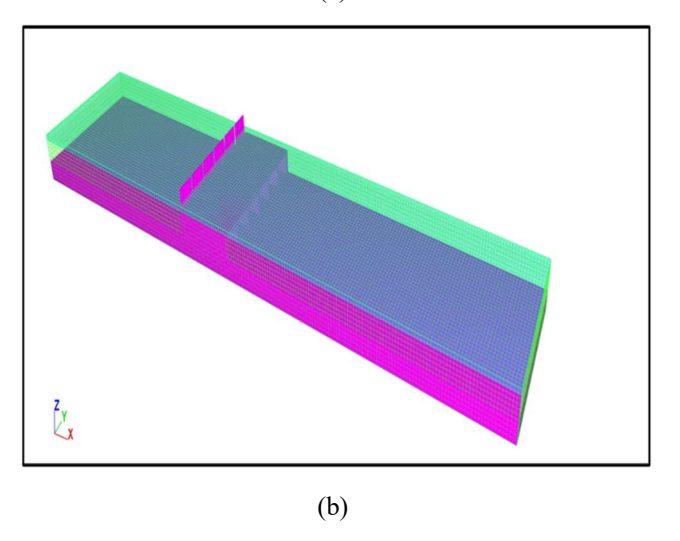


**Figure 1**: Mesh generations by FAVOR<sup>TM</sup>, (a) Fine mesh, (b) Course mesh.

#### 2.7 Conditions at the Boundaries

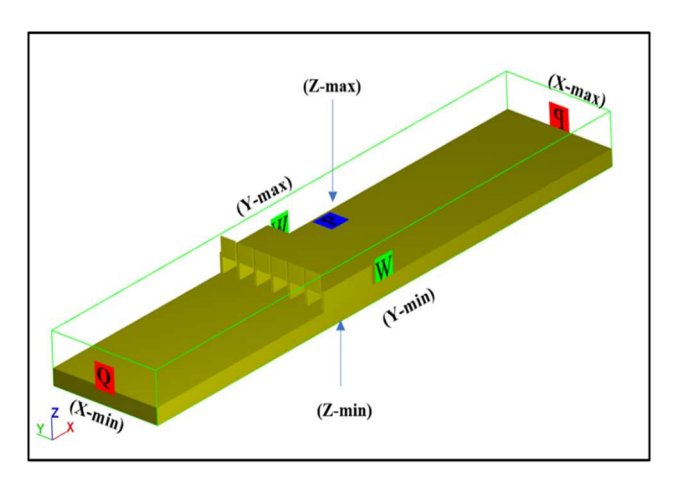
Determining the exact boundary conditions is a crucial step in the numerical simulation process. Accurate alignment of the physical parameters of the investigated situation is necessary. To represent the Cartesian coordinates and determine the 3D flow domain, FlOW-3D employs perpendicular hexahedral meshes. Therefore, it is necessary to build six distinct borders on the rectangular mesh prism. The current study's applied boundary conditions are displayed in **Figure 2**.

Upstream boundary (X-min): An inflow condition Qin. The downstream boundary (X-max) is the specified pressure condition.

Upper limit (Z-max): Pressure state (P).

Lower limit (Z-min): Wall state (W).

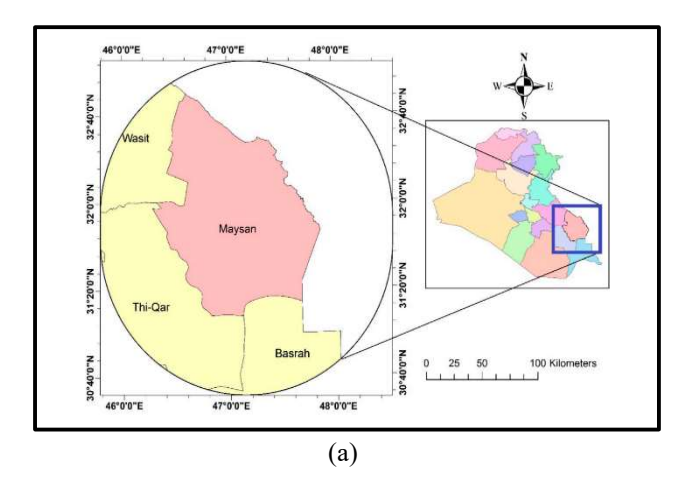
Side boundary: Wall condition (W) (Y-min, Y-max).



**Figure 2**: Boundary conditions for the Al-Kahlaa Regulator.

#### 3. Study area

The Al-Kahlaa Regulator is considered as one of the important Regulator on Tigris River at Mysan Governorate in Iraq. it is located in (31°50'48" N, 47°10'02" E), **Figure 3**. represents the location of the study area.





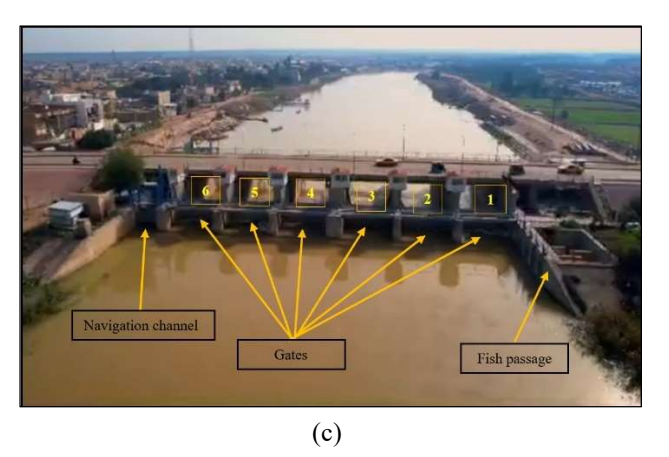


**Figure 3:** (a) Location map of Maysan Governorate [7], (b) Satellite image of study area location (Google Earth, 2024), (c) Upstream of the Al-Kahlaa Regulator, 2024.

#### 4. Field Measurements

The field data were collected with the help of the Amara Barrage Project and the Maysan Irrigation Directorate, which includes the dimensions of the regulator, and everything related to the gates, such as dimensions, number, and the distance between each two gates. In addition to measuring the discharge **Table 1** explains the attributes of the Al-Kahlaa Regulator.

Table 1: Information of the Al-Kahlaa Regulator [18].

No. of gates	width of gate (m)	Pier width (m)	Pier Height (m)	Pier Length (m)	Bed level(m)	Crest level (m)	Stilling basin length (m)	d <sub>50</sub> (mm)
6	8	1.5	8	30	+2	+3	50	0.23

# 5. Calibration of the Al-Kahlaa Regulator model

The calibration process involved a range of discharges, from 39 to 72 m³/s for several scenarios of gate operation, and the mesh with an adequate cell size is crucial for achieving accurate results in numerical simulation, particularly in the context of scouring. Nevertheless, the simulation time's efficiency must also be taken into account due to the substantial quantity of cells. Therefore, the calibration process involved a range of different cell sizes selected as (1, 0.75, 0.5, 0.3, and 0.20) m to identify the best cell size that satisfies the phenomenon conditions. The maximum cell size of 0.3 m was used in this mathematical model .The conditions at the boundaries for all models were set as, the upstream boundary is the inflow

condition Qin, the downstream boundary is the specified pressure condition (P), the upper limit is the pressure state (P), and lastly, the lower limit and the sides boundary (Y-min and Y-max) are set as the wall condition (W).

## 6. Validation of the Al-Kahlaa Regulator model

The simulations reported here are conducted using CFD. At the Al-Kahlaa River, field measurements were made using the River Surveyor M9 flow rate measuring device for the purpose of the validation, **Figure 4**. The samples collected from two parts near the Al-Kahlaa Regulator. The first segment, S1, was taken 300 m upstream of the regulator, while the second section, S2, was obtained 150 m downstream of the regulator, as depicted in **Figure 3(b)**. The riverbed's cross sections are depicted in **Figure 5**. In order to verify the cross-section and flow characteristics of the Al-Kahlaa Regulator, a comparison was made between the mean velocity calculated using a mathematical model and the mean velocity obtained from field measurements at the Al-Kahlaa River.



Figure 4: River Surveyor M9.

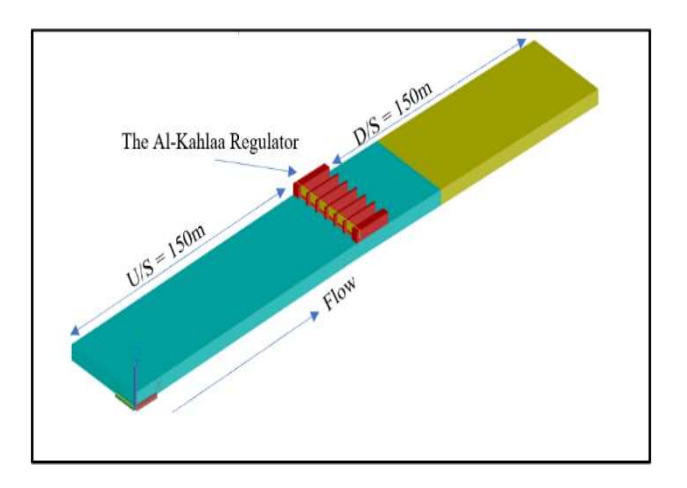


**Figure 5**: Geometry and riverbed of the Al- Kahlaa Regulator (Auto CAD-3D).

# 7. Numerical Simulation for the Al- Kahlaa Regulator

This section describes an examination of a regulator that has six gates located in a rectangular channel. The bed of the canal is moveable and level, with a fixed height of seven meters. The investigation was conducted using CFD simulation. The model's 3D solid shape, as previously stated, is drawn using the AutoCAD-3D modeling tool, and the geometry used in the simulations is exported as a stereolithographic (.stl) format that can be recognized by Flow 3D. To examine the influence of gates opening on scour, the gates have been assigned numerical values spanning from G1 to G6. The flow rate in this investigation varies between 50 and 200 m<sup>3</sup>/s. A uniform grain size of the sand bed was consistently employed for all instances of the gate opening. The regulator's design, number of gates, and dimensions closely resemble those of the Kahlaa Regulator. The channel features, including the flow rate, have been modelled after the Tigris River reach leading to the regulator in Kahlaa Regulator district, as shown in Figure 5. There are 300 m of open channel in total, with 150 m placed upstream of the regulator. The waterway has a width of 70 m and a height of 8 m.

This research has assessed the situations by considering the total number of gates that were opened and the precise order in which they were opened. The cases were divided into six groups, with a total of Thirty-three cases to study the effect of operating the gates with a constant discharge for all cases, and then the worst case was chosen from each group to study the effect of the flow rate. i.e., in case G2 (1,2), the first number indicates the number of open gates, while the number in parentheses indicates the open gate number. In this case, the number of open gates is only two, namely Gate No. 1 and Gate No. 2, where the gates are numbered from right to left. State G6 indicates that all gates are open, and so on for all states. **Table 2**. shows the cases studied in this research.

The mesh, with an adequate cell size, is crucial for achieving accurate results in numerical simulation, particularly in the context of scouring. Nevertheless, the simulation time's efficiency must also be taken into account due to the substantial quantity of cells. The maximum cell size of 0.3 m was used in this mathematical model, the limits for all models were set to match those of the validation model used in the earlier simulation. Except for flow rate, the field-measured value was set and changed in all cases with values ranging from 50–200 m<sup>3</sup>/s to investigate the impact of increasing it on the Scour depth. In this numerical investigation, the validation model is utilised to address sediment scour and turbulence setup. However, additional factors such as the composition of sediment and the average size of particles d50, and sand density.

**Table 2**: Pattern and operation scenarios for the Al-Kahlaa Regulator.

			number		
No.	No.fo	The case	of open	gate number	
1,0,	Group	1110 00.00	gates		
1		G1(1)	1	1	
2	1	G1(2)	1	2	
3		G1(3)	1	3	
4		G2(1,2)	2	1,2	
5		G2(1,3)	2	1,3	
6		G2(1,4)	2	1,4	
7		G2(1,5)	2	1,5	
8	2	G2(1,6)	2	1,6	
9		G2(3,4)	2	3,4	
10		G2(2,5)	2	2.5	
11		G2(2,3)	2	2,3	
12		G2(2,4)	2	2,4	
13		G3(1,2,3)	3	1,2,3	
14		G3(1,5,6)	3	1,5,6	
15		G3(2,5,6)	3	2,5,6	
16		G3(2,3,4)	3	2,3,4	
17	3	G3(1,3,5)	3	1,3,5	
18		G3(1,3,4)	3	1,3,4	
19		G3(2,4,5)	3	2,4,5	
20		G3(1,4,5)	3	1,4,5	
21		G3(1,4,6)	3	1,4,6	
22		G4(1,2,3,4)	4	1,2,3,4	
23		G4(2,3,4,5)	4	2,3,4,5	
24		G4(1,2,5,6)	4	1,2,5,6	
25	4	G4(1,3,4,6)	4	1,3,4,6	
26	4	G4(1,3,4,5)	4	1,3,4,5	
27		G4(1,4,5,6)	4	1,4,5,6	
28		G4(2,3,5,6)	4	2,3,5,6	
29		G4(2,4,5,6)	4	2,4,5,6	
30		G5(1,2,3,4,5)	5	1,2,3,4,5	
31	5	G5(1,3,4,5,6)	5	1,3,4,5,6	
32		G5(1,2,4,5,6)	5	1,2,4,5,6	
33	6	G6	6	1,2,3,4,5,6	

#### 8. Results and Discussion

The following part showcases the outcomes achieved through the utilization of Flow-3D software. This section analyzes the influence of the opening of gates in relation to each other and the rate at which water flows on the maximum depth of scouring.

#### 8.1 Validation Results

To statistically validate the match extent between the results obtained from the Flow-3D software and the field measurements, which examined similar shapes under the same hydraulic conditions. a statistical indicator, such as a Nash-Sutcliffe Efficiency (NSE) test, and the correlation coefficient R<sup>2</sup> was used, where a comparison was made of the mean velocity values that were measured in the field with the mean velocity values calculated by using the mathematical model. The statistical results, which were as follows, NSE value 0.94 and R<sup>2</sup> value 0.9413, indicate that the results of the mathematical model closely match the field measurement with a maximum percentage of difference of 5.88%. The mean velocity calculated from the mathematical model (Vc) and the mean velocity computed from the field measurements (Vf) downstream of the Al-Kahlaa Regulator are shown in Table 3 and Figure 6.

**Table 3**: Vcalculated and Vfield for several scenarios of gate operation for Al-Kahlaa Regulator.

81							
Q U/S (Qin m <sup>3</sup> /s)	Vf(m/s)	Vc(m/s)	No. of open gates	Percente of differene			
39.66	0.186	0.185	2	0.54%			
49.21	0.262	0.256	3	2.30%			
54.2	0.255	0.24	4	5.88%			
68.1	0.2	0.21	5	5%			
72.32	0.29	0.3	6	3.45%			

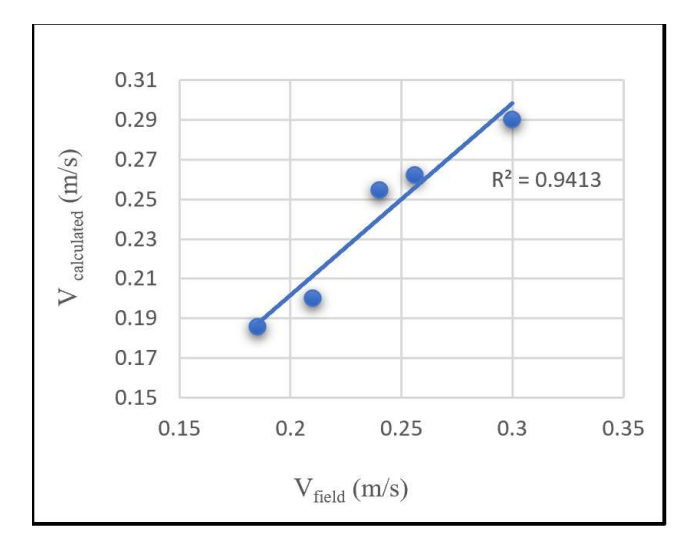


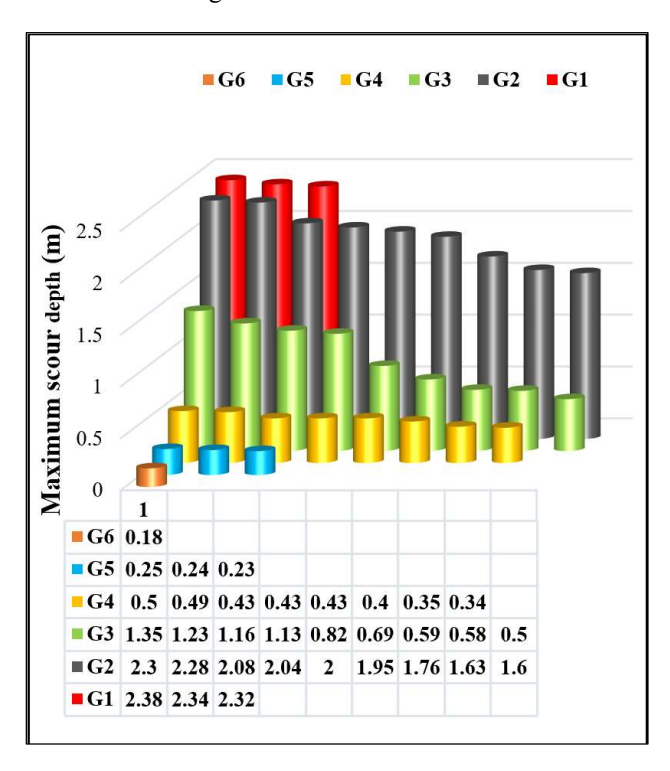
**Figure 6:** calculated and measured mean velocity for Verification of the Al-Kahlaa Regulator model.

## 8.2 The impact of gate operation on the maximum scour depth

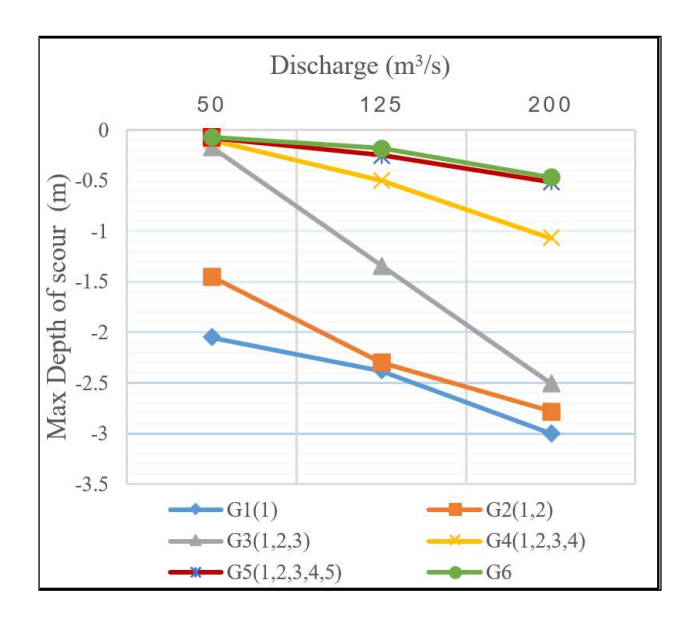
The bar chart in **Figure 7** shows the maximum scouring depth downstream of the Regulator for different gate operation scenarios, maintaining a constant flow rate of 125 m<sup>3</sup>/s. The depth of scouring in case G1(1) is thirteen times greater than in case G6 and more than in case G1(3) once and 2.5%, despite identical open gates. The number of gates opening and their operation directly controls the depth of the scour. Asymmetrical action significantly affects the depth of scouring; when the number of open gates decreases and gates operate unequally, this leads to erosion depth increasing. The results show that sequential operation of the gates on one side leads to the largest scour value, while the best operating condition is when the gates are opened in a non-sequential manner. The results show that they are consistent with the results of previous studies in terms of the best scenarios for gate operation, which are avoiding sequential gate operation and avoiding opening gates on the sides only.

#### 8.3 Influence of flow rate on the scour depth

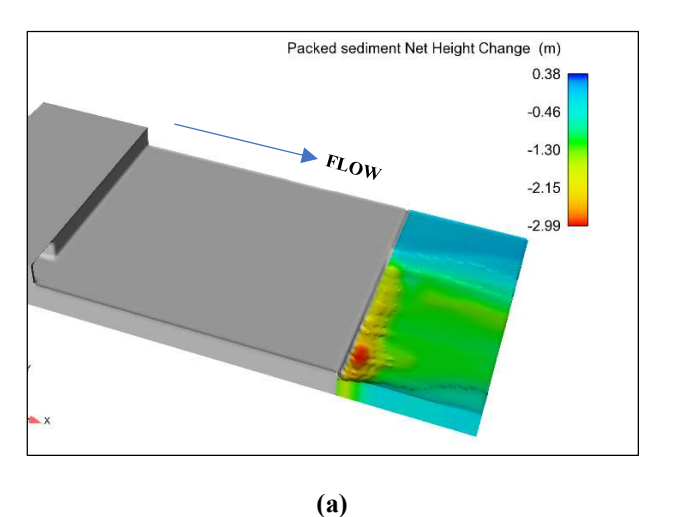
As mentioned above, the worst case was chosen from each group to study the effect of the flow rate. **Figure 8** Illustrates the impact of increasing the rate of flow on the maximum scour depth. It is clear to note that the increase in discharge is small if all gates are open, while the effect is rapid and significant if the number of open gates is reduced. **Figure 9** states the best and worst operating conditions of the gates when the flow rate is 200 m<sup>3</sup>/s.



**Figure 7**: The maximum scour depth for various scenarios of gate operation with a constant flow rate.



**Figure 8**: Relationship between flow rates and maximum scour depth.



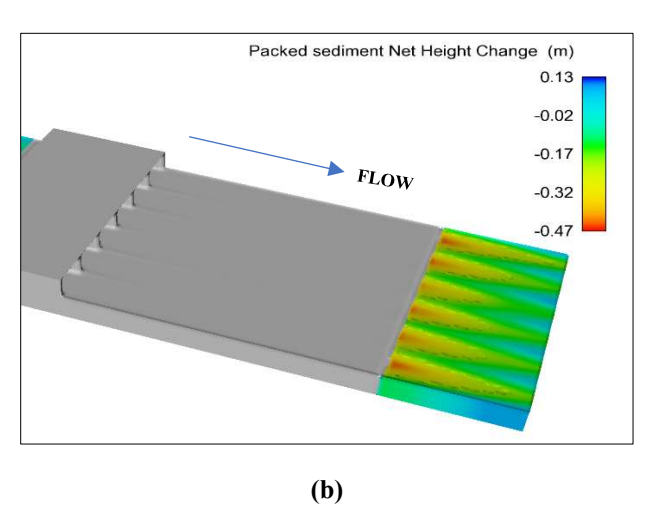


**Figure 9**: The topography of the scour. (a) case G1(1) worst operating, (b) case G6 best operating.

#### 9. Conclusion

This paper focuses on simulating the movement of sediment downstream from the Al-Kahlaa Regulator. Flow-3D software simulations were performed to examine the impact of gate operations on the maximum scour depth downstream of a structure. The results of this simulations were as follows:

- 1 -The number of gates opening, have a substantial impact on the extent of scour occurring downstream of the regulator. The maximum scour depth value was determined with opening, which was 13 times more compared to the case when all gates were opened at a constant flow rate.
- 2 Opening the unequal gates on one side of the regulator and order of gates opening, as well as the operational mechanism of the gates leads to an increase in scouring depth. The size of the scour hole downstream of the regulator increases in proportion to the number of gates that are opened. The results show that sequential operation of the gates on one side leads to the largest scour value, while the best operating condition is when the gates are opened in a non-sequential manner.
- 3- There is a direct relationship between flow rate and scour depth. As the flow rate increases, the depth and extent of scouring also rise, highlighting the influence of flow rate on erosion severity. overall, its effects great when one gate is opened, but it gradually decreases as the number of open gates increases.

#### 10. Recommendations

The following recommendations and suggestions for future studies:

- 1 -The full operation of the regulator gates is highly recommended as the minimum scour occurs, especially in high discharges during flood season. A larger scour is noticed when one gate is opened, threfore its better to partially open of all gates rather than fully opened just few gates.
- 2 -The reserch recommends avoiding opening gates on one side (asymmetric opening of gates) because these scenarios lead to an increase in the scou sownstream of the regulator.
- 3 -Avoid sequential operation of the gates in case not all gates are open and follow the operating scenario in a non-sequential manner. Were the operation of non-consecutive gates the best, because a more appropriate velocity distribution is produced by operating gates with those scenarios.
- 4- In future studies, the thesis recommends incorporating varied sediment sizes, studying partial open gate operation scenarios, as well as studying the effect of operating gates

on the accumulation of sediments upstream of the regulators.

#### References

- [1] Abdulridha, M.S.A. and Al Thamiry, H.A. (2017), "Hydraulic Analysis of the Samarra-Al Tharthar System", Journal of Engineering, doi: 10.31026/j.eng.2017.04.03.
- [2] Abed, B.S. and Majeed, H.Q. (2020), "The behavior of scouring around multiple bridge piers having different shapes", IOP Conference Series: Materials Science and Engineering, Vol. 745, IOP Publishing, p. 12158.
- [3] Al-Awadi, A.T. and Al-Khafaji, M.S. (2021), "CFD-Based Model for Estimating the River Bed Morphological Characteristics near Cylindrical Bridge Piers Due to Debris Accumulation", Water Resources, Springer, Vol. 48, pp. 763–773.
- [4] Al-Hassani, N.Z. and Mohammad, T.A. (2021), "Impact of the Weir Slit Location, the Flow Intensity and the Bed Sand on the Scouring Area and Depth at the Dam Upstream", Journal of Engineering, doi: 10.31026/j.eng.2021.05.04.
- [5] Al-Jubouri, M., Ray, R.P. and Al-Khafaji, M.S. (2023), "Unraveling Debris-Enhanced Local Scour Patterns Around Non-Cylindrical Bridge Piers: Experimental Insights and Innovative Modeling", Sustainability, MDPI, Vol. 15 No. 22, p. 15910.
- [6] Altawash, M.M. and Al Thamiry, H.A. (2022), "Velocity Patterns inside the Proposed Makhool Dam Reservoir with Different Operation Plans", IOP Conference Series: Earth and Environmental Science, Vol. 1120, IOP Publishing, p. 12015.
- [7] Alwan, I.A., Aziz, N.A. and Hamoodi, M.N. (2020), "Potential water harvesting sites identification using spatial multi-criteria evaluation in Maysan Province, Iraq", ISPRS International Journal of Geo-Information, MDPI, Vol. 9 No. 4, p. 235.
- [8] Brethour, J. (2003), "Modeling sediment scour", Flow Science, Santa Fe, NM.
- [9] Daham, M.H. and Abed, B.S. (2020), "One and Two-Dimensional Hydraulic Simulation of a Reach in Al-Gharraf River", Journal of Engineering, doi: 10.31026/j.eng.2020.07.03.
- [10] FLOW 3D Manual. (2014), FLOW 3D, User's Manual.

- [11] Garg, N.K., Bhagat, S.K. and Asthana, B.N. (2002), "Optimal barrage design based on subsurface flow considerations", Journal of Irrigation and Drainage Engineering, American Society of Civil Engineers, Vol. 128 No. 4, pp. 253–263.
- [12] Hirt, C.W. and Nichols, B.D. (1981), "Volume of fluid (VOF) method for the dynamics of free boundaries", Journal of Computational Physics, Elsevier, Vol. 39 No. 1, pp. 201–225.
- [13] Hyperinfo Corp. (2016), "Flow-3D V11. 2", Flow Science, Inc. Santa Fe, NM, USA.
- [14] Ibrahim, A.K. and AL-Thamiry, H.A.K. (2018), "Experimental Study of Local Scour Around Elliptic and Semi-parabolic Groynes in Straight Channels", Association of Arab Universities Journal of Engineering Sciences, Vol. 25 No. 4, pp. 105–116.
- [15] Jalal, H.K. and Hassan, W.H. (2020), "Three-dimensional numerical simulation of local scour around circular bridge pier using Flow-3D software", IOP Conference Series: Materials Science and Engineering, Vol. 745, IOP Publishing, p. 12150.
- [16] Kumer, H.Q. (2019), Simulation and Evaluation of Scouring Downstream Barrages, M Sc. Thesis University of Wasit /Unpublished.
- [17] Majeed, H.Q., Abed, B.S. and Shamkhi, M.S. (2021), "CFD simulation for the operation effect of gates openings of al-hay regulator on the local erosion", Journal of Engineering Science and Technology, Vol. 16 No. 2, pp. 1098–1109.
- [18] Maysan Irrigation Directorate, (2023), Data of the Hydraulic Information of Structures; Unpublished Data., Vol. 10.
- [19] Meyer-Peter, E. and Müller, R. (1948), "Formulas for bed-load transport", IAHSR 2nd Meeting, Stockholm, Appendix 2, IAHR.
- [20] Mohy, H.M. and Abed, B.S. (2020), "Design of Expert System for Managing the System of AthTharthar Lake", Journal of Engineering, Baghdad University, Vol. 26 No. 1, pp. 142–159.
- [21] Nielsen, P. (1992), Coastal Bottom Boundary Layers and Sediment Transport, Vol. 4, World scientific.
- [22] Nkad, N.Z., Mohammad, T.A. and Hammoodi, H.M. (2022), "Experimental Investigations on

- Scour Volume Upstream of a Slit Weir.", Pertanika Journal of Science & Technology, Vol. 30 No. 3.
- [23] Omara, H. and Tawfik, A. (2018), "Numerical study of local scour around bridge piers", IOP Conference Series: Earth and Environmental Science, Vol. 151, IOP Publishing, p. 12013.
- [24] Rasool, H. and Mohammed, T.A. (2023), "Checking the Accuracy of Selected Formulae for both Clear Water and Live Bed Bridge Scour", Journal of Engineering, Vol. 29 No. 2, pp. 99–111.
- [25] Van Rijn, L.C. (1984), "Sediment transport, part I: bed load transport", Journal of Hydraulic Engineering, American Society of Civil Engineers, Vol. 110 No. 10, pp. 1431–1456.
- [26] S Abbas, A. and I Abdulridha, R. (2016), "Effect of floating debris on local scour at bridge piers", Engineering and Technology Journal, University of Technology-Iraq, Vol. 34 No. 2A, pp. 356–367.
- [27] Smith, L.M. and Woodruff, S.L. (1998), "Renormalization-group analysis of turbulence", Annual Review of Fluid Mechanics, Annual Reviews 4139 El Camino Way, PO Box 10139, Palo Alto, CA 94303-0139, USA, Vol. 30 No. 1, pp. 275–310.
- [28] Soulsby, R. (1997), "Dynamics of marine sands", T. Telford London, UK.
- [29] Wei, G., Brethour, J., Grünzner, M. and Burnham, J. (2014), "The sedimentation scour model in FLOW-3D®", Flow Sci Rep, Vol. 3, pp. 1–29.
- [30] Yakhot, V. and Smith, L.M. (1992), "The renormalization group, the ε-expansion and derivation of turbulence models", Journal of Scientific Computing, Springer, Vol. 7, pp. 35–61.
- [31] Zhang, Q., Zhou, X.-L. and Wang, J.-H. (2017), "Numerical investigation of local scour around three adjacent piles with different arrangements under current", Ocean Engineering, Elsevier, Vol. 142, pp. 625–638.

### تأثير تشغيل البوابات على الحد الاقصى للانجراف مؤخر ناظم الحكلاء

### هادی أمیر عباس ۱٬ ۴٬ حیدر قیس مجید 2

أقسم هندسة الموارد المائية، كلية الهندسة ، جامعة بغداد، بغداد، العراق، Hadi.ameer2310 @coeng.uobaghdad.edu.iq

bmajeed @coeng.uobaghdad.edu.iq - تُغسم هندسة الموارد المائية، كلية الهندسة، جامعة بغداد، بغداد، العراق،

\* الباحث الممثل : هادي أمير عباس، Hadi.ameer2310 @coeng.uobaghdad.edu.iq

نشر في : 30 ايلول 2025

الخلاصة – تعتبر النواظم والهياكل الهيدروليكية الأخرى ضرورية لإدارة الندفق في القنوات المفتوحة. يتم إنتاج أنماط انجراف غير متوقعة عندما يتم تشغيل بوابات هذه الهياكل بشكل غير صحيح. تهدف الدراسة إلى النظر في الأداء الأمثل لبوابات ناظم الكحلاء في العراق، مع التركيز على حركة الرواسب وقضايا الترسيب. في هذا البحث، تم استخدام برنامج Flow-3D، وتحديداً نموذج RNG للجريان المضطرب، لمحاكاة تدفق المياه ونظرية تنظيف الرواسب لمحاكاة حركة الرواسب في ظل ظروف تدفق مختلفة وخيارات فتح البوابة. ووفقا للدراسة، فإن عدد البوابات المفتوحة وكيفية تشغيلها لهما تأثير كبير على كيفية تطور عملية الانجراف في مؤخر الناظم. تم تسجيل اقصى قيمة للانجراف عند فتح بوابة واحدة، وهي 13 مرة أكثر مقارنة بالحالة عند فتح جميع البوابات بمعدل تدفق 125 م³رثانية. من ناحية أخرى، وفي حالة فتح بوابة واحدة تم تسجيل أقصى عمق للانجراف عند 2.05 متر عندما كان معدل التدفق 50 م5/ثانية و 3 متر عند 200 م5/ثانية، أي ما يعادل زيادة و1.1 مرة. وبشكل عام، يتناقص الحد الأقصى لعمق النحر في مؤخر الناظم مع زيادة عدد البوابات المفتوحة.

الكلمات الرئيسية – ناظم الكحلاء، برنامج التدفق ثلاثي الابعاد، التدفق في القنوات المفتوحة، نموذج الجريان المضطرب، الانجراف.